

Chemistry - A European Journal

A Mechanistic Study of the Multiple Roles of Oleic Acid in the Oil-Phase Synthesis of Pt Nanocrystals --Manuscript Draft--

Manuscript Number:	chem.202003202R1
Article Type:	Full Paper
Corresponding Author:	Younan Xia, Prof. Georgia Institute of Technology Atlanta, GA UNITED STATES
Corresponding Author E-Mail:	younan.xia@bme.gatech.edu
Order of Authors (with Contributor Roles):	Younan Xia, Prof. Minghao Xie Zhiheng Lyu Ruhui Chen
Keywords:	oleic acid; nanocrystals; nucleation and growth; platinum
Manuscript Classifications:	Carboxylate ligands; Crystal growth; Nanocrystals; Precursor chemistry
Abstract:	Oleic acid (OAc) is commonly used as a surfactant and/or solvent for the oil-phase synthesis of metal nanocrystals but its explicit roles are yet to be resolved. Here we report a systematic study of this problem by focusing on a synthesis that simply involves heating of Pt(acac) ₂ in OAc for the generation of Pt nanocrystals. When heated at 80 °C, the ligand exchange between Pt(acac) ₂ and OAc leads to the formation of a Pt(II)-oleate complex that serves as the actual precursor to Pt atoms. Upon increasing the temperature to 120 °C, the decarbonylation of OAc produces CO, which can act as a reducing agent for the generation of Pt atoms and thus formation of nuclei. Afterwards, several catalytic reactions can take place on the surface of the Pt nuclei to produce more CO, which also serves as a capping agent for the formation of Pt nanocrystals enclosed by {100} facets. The emergence of Pt nanocrystals further promotes the autocatalytic surface reduction of Pt(II) precursor to enable the continuation of growth. This work not only elucidates the critical roles of OAc at different stages in a synthesis of Pt nanocrystals but also represents a pivotal step forward toward the rational synthesis of metal nanocrystals.
Response to Reviewers:	Dr. Anne Deveson Deputy Editor of Chemistry – A European Journal Dear Anne, Many thanks for your e-mail dated August 3, 2020. We have revised our manuscript by taking into account all the suggestions and comments from you and the two reviewers. All changes are highlighted with yellow pen in the review-only copy of the revised manuscript. Here we would like to specifically address the concerns from the reviewers. Reviewer #1 Recommendation: Publish after minor revisions noted. “In this manuscript, the authors elucidated the systematic study of role with oleic acid (OAc) in the nucleation and growth pathway. This manuscript has intensively investigated the effective role of OAc as a surfactant and reducing agent by FT-IR, UV-visible, TEM analysis, and controlled experiments. They showed that CO can be generated from OAc through a series of chemical reactions such as the dehydrogenation reaction, water-gas shift reaction, and decarbonylation process. As produced CO acts as a reducing agent and a surface stabilizer for (100) facet of Pt. Explaining the mechanism and the role of conventional surfactants is crucial in this field to understand overall nanoparticle synthesis in wet chemistry. Therefore, the paper is

providing many scientific contents that are significant in the community of nanoscience. Below are comments/questions, which can be addressed during the revision process.”

1) “On page 5 in the manuscript, the authors explained that the diversity of the nanocrystal morphologies was ascribed to the multiple nucleation events. Recently, studies have reported that similar issues can be caused by impurities in commercial solvents. The presence of eladic acid, conformation isomer of OAc, can result in the inhomogeneity of nanocrystal morphology. It might be worth citing a recent report from Jonas and coworkers discussing the influence of impurity of commercial solvents. (Chem. Mater., 2019, 31, 4, 1223-1230).”

Response: We thank the reviewer for raising an excellent point. We have added the discussion and cited the reference about the potential impact of impurities in commercial solvents on the diversity of the nanocrystals to the revised manuscript (see page 5 and ref. 11b).

2) “The results for the reaction of Pt under OAc is intriguing. The authors showed that CO generated from OAc can trigger the reduction of Pt precursor. Despite the evidence for the specific steps with FT-IR, I suggest the author test at least a few other possible metal precursors here to show more cases. The authors mentioned the synthesis of Pd nanocrystals according to the previous reports of reference [3b]. However, the solvent in reference [3b] is not the OAc, but ethylene glycol.”

Response: We thank the reviewer for the constructive suggestion. We have used other metal precursors including Pd(acac)₂ and Ir(acac)₃ under the same experimental condition and collected the FTIR spectra of the resultant Pd and Ir nanocrystals to confirm the generation and adsorption of CO. We have added the discussion to the revised manuscript (see page 12), together with the TEM and FTIR data to the Supporting Information as Figure S3 and S4.

For the reference 3b, although it reports the synthesis of Pd nanocrystals in ethylene glycol, the conclusion about the relationship between the initial reduction rate of the PdII precursor and the internal structure of the Pd seeds should be universal for the synthesis of noble-metal nanocrystals under different experimental conditions.

3) “On page 10, The authors mentioned that the stretching mode of =C-H in Figure S2 decreased after the reaction at 80 oC. However, there is no corresponding data shown at 80 oC but only 120 oC in Figure S2. Therefore, the argument of the stretching modes is somewhat inconsistent.”

Response: We thank the reviewer for his/her careful examination of our manuscript. We have corrected the inconsistent description in the revised manuscript (see page 10).

4) “The description of the decomposition mechanism of OAc on page 10 should be reconsidered and revised. The authors mentioned that “Under the experimental conditions, the H₂ gas can only be generated through the decarbonylation of OAc, followed by water-gas shift reaction”. In the cited reference with Table 1, H₂ gas is generated through water-gas shift reaction rather than the decarbonylation of OAc. It is somewhat inconsistent that makes it hard to grab the key points of the mechanism.”

Response: We understand the concern of this reviewer. Under the experimental condition of the present work, the H₂ gas can only be generated through water-gas shift reaction, which requires CO and H₂O as the reactants. Since the initially added chemicals only included Pt(acac)₂ and OAc, the CO and H₂O can only be produced through the decarbonylation of OAc. Therefore, we argued that decarbonylation of OAc led to the formation of H₂ gas, which is responsible for the subsequent hydrogenation of OAc.

Reviewer #2

Recommendation: Publish as is; no revisions needed.

	<p>“This paper described a detailed and systematic study on the role of Oleic acid (OAc) on the synthesis of Pt nanocrystals. The results reported in this paper are important because it elucidates critical mechanistic aspects related to the role of OAc during the nucleation and growth stages of the synthesis, paving the way to the development of improved strategies for the tightly controlled synthesis of nanocrystals with target sizes and shapes. I believe the paper is of high quality and significance. It is also well written and the discussion is appropriately supported by the data. I recommend publication as it is.”</p> <p>Response: We thank the reviewer for his/her candid assessment of our work.</p> <p>We have also made some additional editorial changes to further enhance the quality of our paper. It is hoped the revised manuscript is now in the right format for publication in Chemistry – A European Journal.</p> <p>Sincerely yours, Younan Xia</p>
Section/Category:	
Additional Information:	
Question	Response
Do you agree to comply with the legal and ethical responsibilities outlined in the journal's Notice to Authors?	Yes
Has a previous version of this manuscript been submitted to this journal?	No
Is this manuscript, or part of it, currently under consideration elsewhere?	No
Is this manuscript, or part of it, published, posted, or in press? This includes content posted on preprint servers (preprint guidelines) or published as part of a thesis.	No
Please provide us with information about the history of your manuscript, including previous submissions, transfers, or prior versions:	This material has not been published and is not under consideration for publication elsewhere.
Do you or any of your co-authors have a conflict of interest to declare?	No
Does the research described in this manuscript include animal experiments or human subjects or tissue samples from human subjects?	No

Revised MS# chem.202003202

A Mechanistic Study of the Multiple Roles of Oleic Acid in the Oil-Phase Synthesis of Pt Nanocrystals

Minghao Xie,^[a] Zhiheng Lyu,^[a] Ruhui Chen,^[a] and Younan Xia^{*[a,b]}

[a] M. Xie, Z. Lyu, R. Chen, Prof. Dr. Y. Xia

School of Chemistry and Biochemistry,

Georgia Institute of Technology

Atlanta, Georgia 30332 (USA)

E-mail: younan.xia@bme.gatech.edu

[b] Prof. Y. Xia

The Wallace H. Coulter Department of Biomedical Engineering

Georgia Institute of Technology and Emory University

Atlanta, Georgia 30332 (USA)

Supporting information for this article is given via a link at the end of the document.

Abstract

Oleic acid (OAc) is commonly used as a surfactant and/or solvent for the oil-phase synthesis of metal nanocrystals but its explicit roles are yet to be resolved. Here we report a systematic study of this problem by focusing on a synthesis that simply involves heating of $\text{Pt}(\text{acac})_2$ in OAc for the generation of Pt nanocrystals. When heated at 80 °C, the ligand exchange between $\text{Pt}(\text{acac})_2$ and OAc leads to the formation of a Pt^{II} -oleate complex that serves as the actual precursor to Pt atoms. Upon increasing the temperature to 120 °C, the decarbonylation of OAc produces CO, which can act as a reducing agent for the generation of Pt atoms and thus formation of nuclei. Afterwards, several catalytic reactions can take place on the surface of the Pt nuclei to produce more CO, which also serves as a capping agent for the formation of Pt nanocrystals enclosed by {100} facets. The emergence of Pt nanocrystals further promotes the autocatalytic surface reduction of Pt^{II} precursor to enable the continuation of growth. This work not only elucidates the critical roles of OAc at different stages in a synthesis of Pt nanocrystals but also represents a pivotal step forward toward the rational synthesis of metal nanocrystals.

Introduction

Colloidal metal nanocrystals have been extensively investigated in recent years because of their remarkable properties for a variety of applications including catalysis, photonics, electronics, and medicine.^[1] For most of these applications, it is necessary to have a tight control over the size, shape, and internal structure of the nanocrystals in order to optimize their properties and thereby enhance their performance.^[2] The synthesis of colloidal metal nanocrystals typically involves the reduction of a salt precursor, followed by the nucleation and growth of the resultant atoms. In order to obtain nanocrystals with controlled sizes, shapes, and internal structures, one has to pay close attention to the chemical reagents involved in a synthesis, including the salt precursor, reducing agent, capping agent, and colloidal stabilizer.^[3] It is the interplay among these reagents that defines the thermodynamic and kinetic conditions directly affecting the nucleation and growth of metal nanocrystals.^[4]

Among various metals, Pt is extensively utilized in industry as a catalytic material for a wide variety of applications, including the oxygen reduction reaction (ORR) in fuel cells.^[5] It is well-established that the catalytic performance of Pt nanocrystals can be enhanced by tuning their size, shape, and/or internal structure.^[6] To date, there are a large number of reports on the colloidal synthesis of Pt nanocrystals with diverse shapes and internal structures.^[7] Among them, oil-phase synthesis easily stands out as one of the most commonly used protocols for the production of Pt colloidal nanocrystals with uniform and tunable sizes and shapes.^[8] Most of the reported protocols involved the use of oleylamine (OAm) or oleic acid (OAc) owing to its ability to adsorb onto the surface of the nanocrystals and thereby affect their shape evolution. In addition, these molecules may also coordinate with the metal ions, generating intermediate complexes featuring reduction kinetics different from that of the original precursor.^[9] For example, Yang and co-workers proved that both primary aliphatic amine and carboxylic acid could serve as coordination ligands to Pt^{II} ions through metal-ligand complexation.^[10] The multiple roles played by OAm, either alone or in combination with other reactants, have been extensively studied, and it is generally accepted that it can serve as a solvent, a surfactant, and a reducing agent depending on the exact experimental

conditions.^[9,11] To our knowledge, a molecular-level understanding of the roles played by OAc alone in the synthesis of Pt nanocrystals is still missing because it is usually used in combination with other chemicals. As a long-chain fatty acid with a double bond in the middle, OAc has the capacity to play multiple roles in a colloidal synthesis of Pt nanocrystals. For example, the carboxylic acid group can coordinate with Pt^{II} ions and act as an electron donor at an elevated temperature. The unsaturated aliphatic chain can effectively passivate the surface of Pt nanocrystals and thus prevent them from aggregation. In principle, it is feasible to generate Pt nanocrystals from a Pt^{II} precursor in the presence of OAc only, without the need to introduce any other chemical reagent.

Herein, we report a systematic study of the roles played by OAc in the nucleation and growth of Pt nanocrystals. The synthesis simply involves the heating of Pt(acac)₂ in OAc. The reaction mixture is heated at 80 °C for the generation of a Pt^{II}-oleate complex through ligand exchange. When continued with heating at a higher temperature, Pt cubes/bars are obtained, together with a small fraction of right bipyramids and penta-twinned nanorods. Our time-elapse studies indicate that primary and secondary nucleation events resulted in the formation of single-crystal and twinned seeds, respectively, followed by their growth through an Ostwald ripening mechanism. Our analyses demonstrate that OAc plays distinctive roles at different stages of the synthesis. In the pre-nucleation stage at 80 °C, OAc undergoes ligand exchange with Pt(acac)₂ to generate a trimeric Pt^{II} precursor. Upon entering the nucleation stage at a higher temperature, decarbonylation of OAc produces CO as a strong reducing agent for the generation of Pt atoms and induction of homogeneous nucleation. Once Pt seeds have been formed, OAc can serve as a colloidal stabilizer by forming a densely-packed layer on their surface. At this point, several catalytic reactions can take place on the surface of Pt for the production of more CO to serve as a capping agent toward Pt{100} facets and thus promote the formation of Pt cubes/bars as the major product. The Pt nanocrystals can facilitate the autocatalytic, surface reduction of Pt^{II} precursor to ensure their continuous growth. The size and shape of the Pt nanocrystals can be tailored by varying the reaction temperature and/or the molar ratio between Pt(acac)₂ and OAc.

Results and Discussion

Synthesis of Pt Nanoscale Cubes/Bars. In a typical protocol, $\text{Pt}(\text{acac})_2$ was dissolved in OAc at 80 °C and then reduced at a higher temperature. The solution gradually turned from bright yellow to dark brown and finally black, indicating the formation of Pt nanocrystals. Figure 1a shows a typical transmission electron microscopy (TEM) image of the as-obtained Pt nanocrystals dominated by nanoscale cubes/bars with a purity of about 70%. The purity was estimated by analyzing 50 particles in the same sample. In addition to the single-crystal cubes/bars, the product also contained other types of nanocrystals, including those with singly- and multiply-twinned structures. The cubes had an average edge length of 10 nm while the bars had an average shorter edge length of 8 nm and an aspect ratio of 1.7. Figure 1b shows TEM images of individual nanocrystals marked in Figure 1a, including cube, bar, right bipyramid, and pentagonal nanorod. The diversity of the nanocrystals likely arose from the involvement of multiple nucleation events and thus the formation of seeds featuring different types of internal structures and distinct shapes. Additionally, the presence of elaidic acid, a typical impurity in the as-received OAc with a purity of 90%, might also contribute the inhomogeneity observed for the nanocrystals.^[11b] The X-ray diffraction (XRD) pattern shown in Figure S1 confirmed that the as-synthesized Pt nanocrystals took a face-centered cubic (*fcc*) structure identical to that of bulk Pt. The intensity ratio between the peaks of (200) and (111) diffraction was increased relative to that of the bulk sample (JCPDS #03-2557), suggesting the increased orientation of nanocrystals along <100> direction. This result further confirms that the product was dominated by Pt cubes/bars enclosed by {100} facets and thus preferentially orientated along <100> direction when deposited on the substrate for XRD.

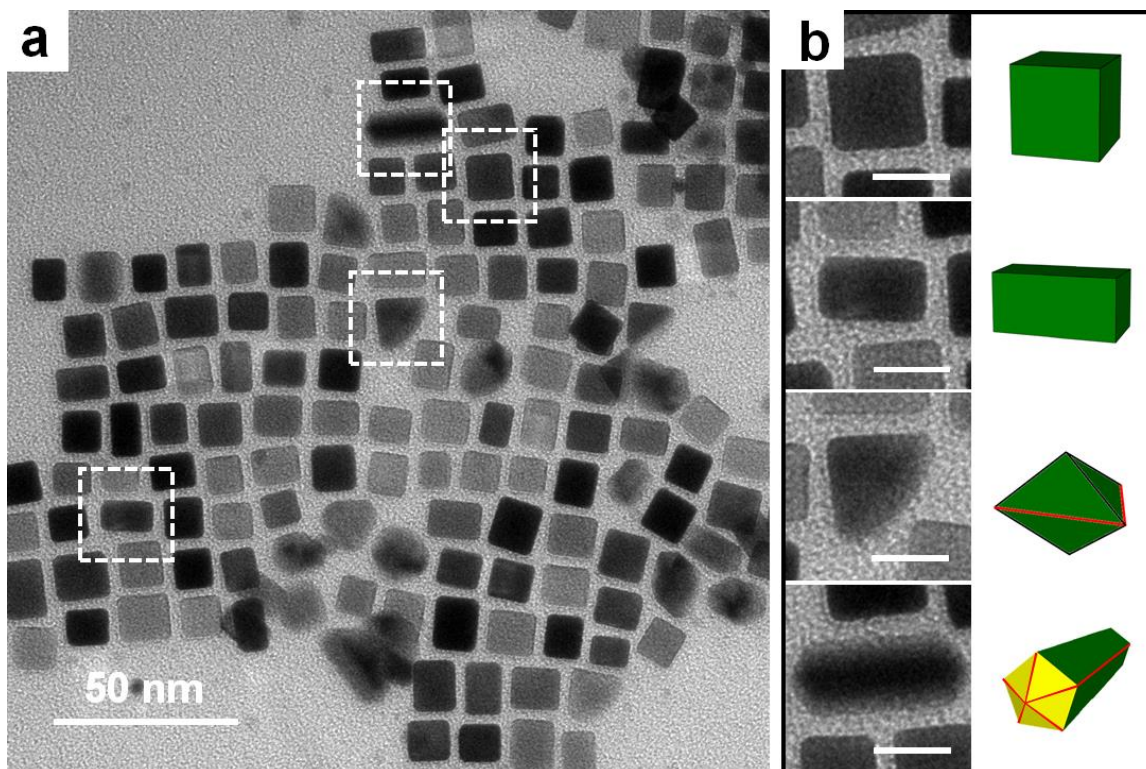


Figure 1. (a) A typical TEM image of the Pt nanocrystals synthesized using 90% OAc. (b) TEM images and the corresponding models of Pt nanocrystals in the shapes of cube, bar, right bipyramid, and penta-twinned nanorod, respectively. The scale bars are 10 nm.

To elucidate the growth mechanism, solid products were sampled from the reaction solution of a standard synthesis at different time points and analyzed using TEM. In the early stage ($t=1$ h, [Figure 2a](#)), small seeds with a broad distribution in size (1–5 nm) were formed, together with some truncated cubes/bars (cubes: 8 nm in edge length; bars: 6 nm in shorter edge length and an aspect ratio of 1.5). When the reaction time was prolonged to $t=6$ h ([Figure 2b](#)), the seeds were increased in size, together with the emergence of a larger portion of truncated cubes/bars. As the synthesis was prolonged, more seeds grew into nanocrystals with a single-crystal structure, including truncated cubes/bars, cuboctahedra, and truncated octahedra. As shown in [Figure 2c](#) ($t=12$ h), there still existed some tiny seeds with sizes below 2 nm, indicating an additional nucleation event at the late stage of a synthesis. At $t=24$ h ([Figure 2d](#)), the product was dominated by Pt cubes/bars,

together with some newly emerged nanocrystals featuring a singly- or multiply-twinned structure. A comparison of the products obtained at $t=12$ h and 24 h indicates that the growth of the cubes/bars was mainly driven by Ostwald ripening, in which the Pt atoms were dissolved from smaller seeds and redeposited onto the growing cubes/bars to further increase their sizes. Further extension of the reaction time beyond 24 h did not result in any apparent changes to the distributions in both size and internal structure.

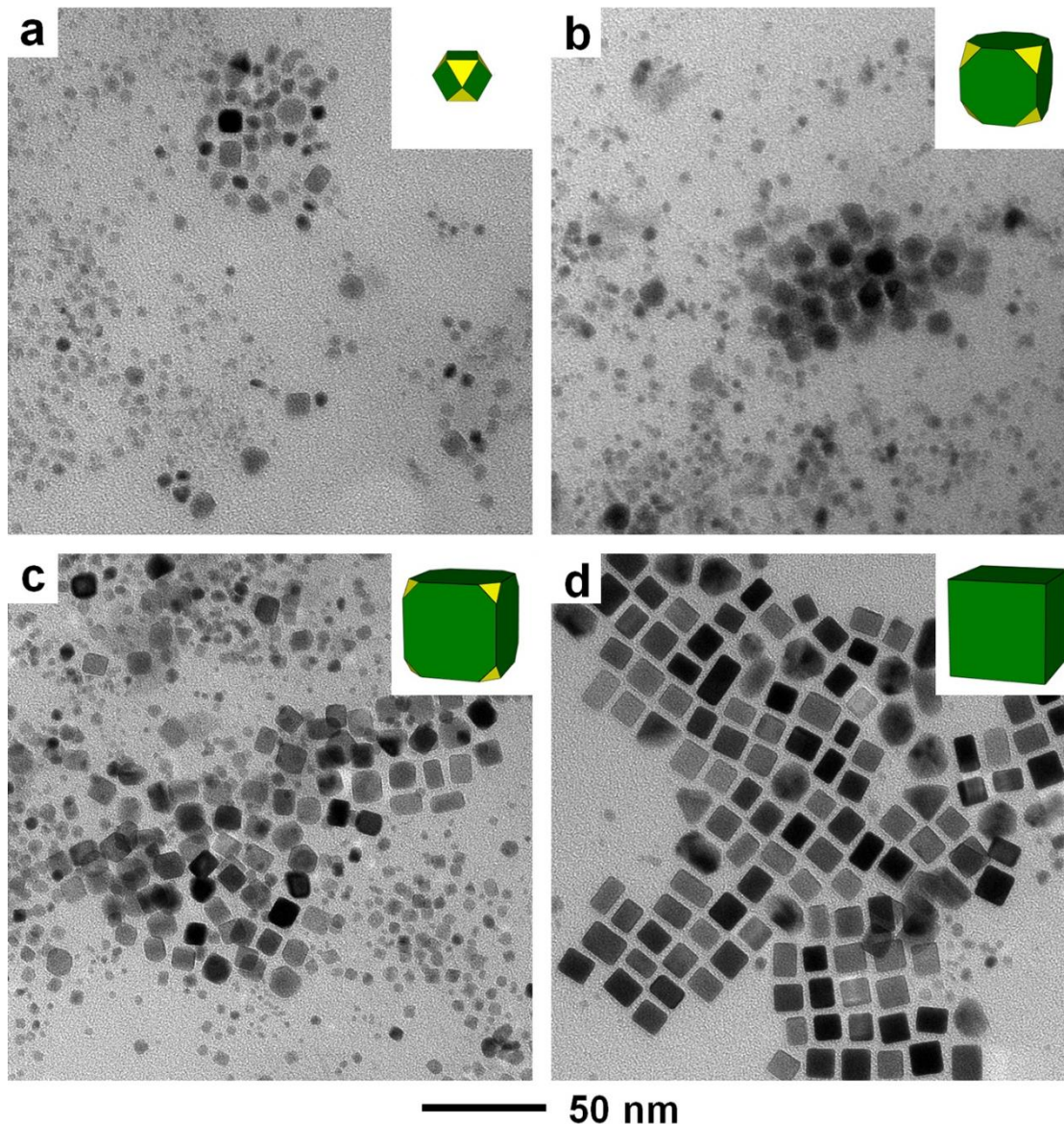


Figure 2. TEM images of Pt nanocrystals obtained at different time points of a standard synthesis: (a) 1, (b) 6, (c) 12, and (d) 24 h. The models in the insets indicate the dominant nanocrystals in the products.

Nucleation and Growth. Based on the results in Figure 2 and the LaMer model, we proposed a plausible mechanism to account for the nucleation and growth of Pt nanocrystals (Figure 3). Overall, the synthesis followed the LaMer model with some minor modifications. At the beginning (stage I), the concentration of Pt atoms steadily increased with time due to the reduction of the Pt^{II} precursor. Once the concentration of Pt atoms passed the minimal level for self-nucleation (C_{min}^{nu}), the Pt atoms started to aggregate into nuclei *via* homogeneous nucleation (stage II). In this stage, the reduction rate of Pt^{II} was relatively fast, producing a large number of nuclei in the solution. Once formed, the nuclei could grow in an accelerated manner, quickly decreasing the concentration of Pt atoms to a level below C_{min}^{nu} . In the first half of stage III, a portion of the nuclei grew into larger sizes, further consuming Pt atoms and depleted their concentration to a lower level. However, the generation of Pt atoms by continuous reduction could push the concentration of Pt atoms to a level over C_{min}^{nu} again, entering a secondary nucleation stage (stage IV). In this stage, although the atomic concentration was high, the reduction rate of Pt^{II} became much slower relative to that in stage II due to the consumption of Pt^{II}.^[3b] As a result, the newly produced seeds tended to contain singly- and multiply-twinned structures. This proposed mechanism is consistent with one of our previous study about the relationship between the initial reduction rate of Pd^{II} precursor and the internal structure of the newly formed Pd seeds.^[3b] After secondary nucleation, most of the Pt^{II} was consumed and the atomic concentration dropped below C_{min}^{nu} to enter stage V for growth only. In this stage, the twinned seeds could grow into right bipyramids and penta-twinned nanorods, while the single-crystal seeds evolved into cubes/bars.

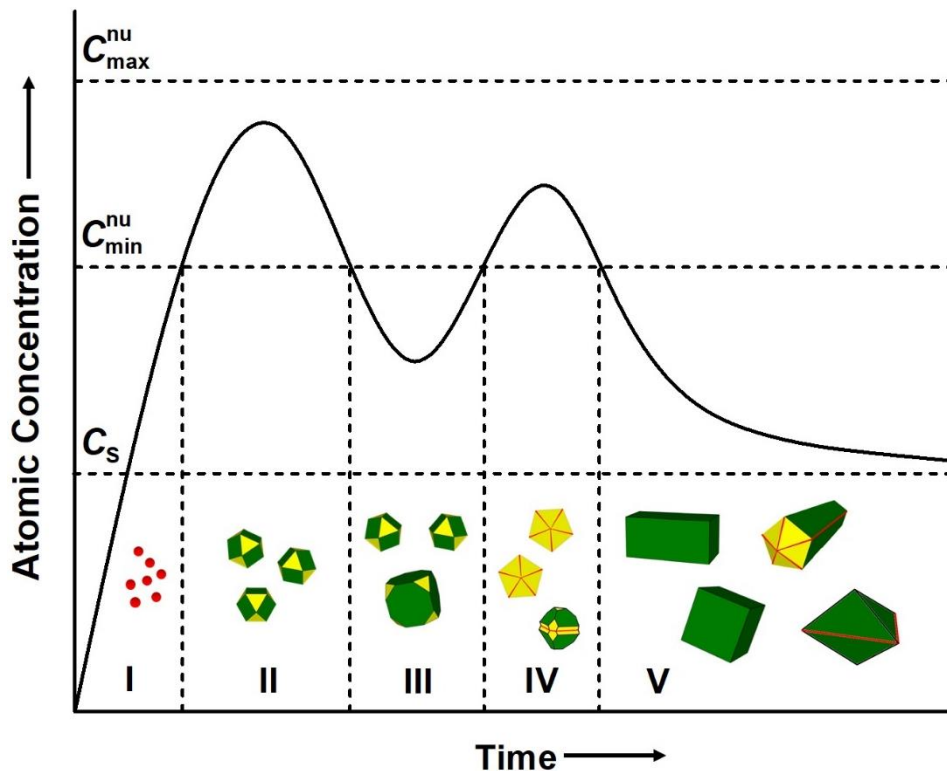


Figure 3. Schematic illustration of the nucleation and growth processes involved in the synthesis of Pt nanocrystals according to the LaMer model. Stages I, II, III, IV, and V correspond to the initial generation of atoms, primary nucleation, growth, secondary nucleation, and growth, respectively.

The Multiple Roles Played by OAc. As noted above for the synthesis of Pt nanocrystals in OAc, the Pt^{II} precursor was firstly reduced to Pt atoms, followed by aggregation into nuclei/seeds and finally growth into nanocrystals. In order to figure out the roles played by OAc at different stages of such a synthesis, we firstly examined the interaction between $\text{Pt}(\text{acac})_2$ and OAc in the pre-nucleation stage using ultraviolet–visible (UV–vis) spectroscopy. Figure 4a shows the UV–vis spectra recorded from different solutions prepared from $\text{Pt}(\text{acac})_2$. For the $\text{Pt}(\text{acac})_2$ dissolved in ethanol, it displayed a strong absorption peak at 344 nm, corresponding to the Pt^{II} –acetylacetonate complex.^[12] However, this peak disappeared when $\text{Pt}(\text{acac})_2$ was dissolved in OAc at 80 °C, indicating the coordination of OAc to Pt^{II} ions for the formation of a Pt^{II} –oleate complex. Based on previous studies about Pd/Pt–carboxylate complexes, the Pt^{II} –oleate complexes might

1
2
3
4
5 exist in a trimeric structure, with each of the Pt^{II} ions coordinating with four oxygen atoms to give
6
7 a formula of Pt₃(OAc)₆ for the actual precursor.^[13] The as-formed trimeric Pt^{II} clusters could be
8
9 stabilized by OAc at 80 °C during the pre-nucleation stage. Once heated to a higher temperature
10
11 such as 120 °C, OAc went through a decarbonylation process in the presence of Pt^{II} complex for
12
13 the production of CO. To confirm this process, we measured the Fourier-transform infrared (FTIR)
14
15 spectra of OAc heated at 120 °C for different periods of time (Figure S2). In the absence of
16
17 Pt(acac)₂, the FTIR spectra did not change after heating for 24 h. In contrast, the intensity of the
18
19 stretching mode of =C–H (3005 cm⁻¹) for OAc in the presence of Pt(acac)₂ (at a molar ratio of
20
21 5714 between OAc and Pt(acac)₂) decreased with time when heated at 120 °C, indicating the
22
23 hydrogenation of OAc and thus the presence of H₂ in the system. Under the experimental condition,
24
25 the H₂ gas can only be generated through the decarbonylation of OAc, follow by water-gas shift
26
27 reaction.^[14] The CO produced through decarbonylation could serve as a reducing agent, converting
28
29 the Pt^{II} precursor to Pt atoms for the induction of homogeneous nucleation.
30
31
32
33
34
35
36
37
38
39
40
41
42
43
44
45
46
47
48
49
50
51
52
53
54
55
56
57
58
59
60
61
62
63
64
65

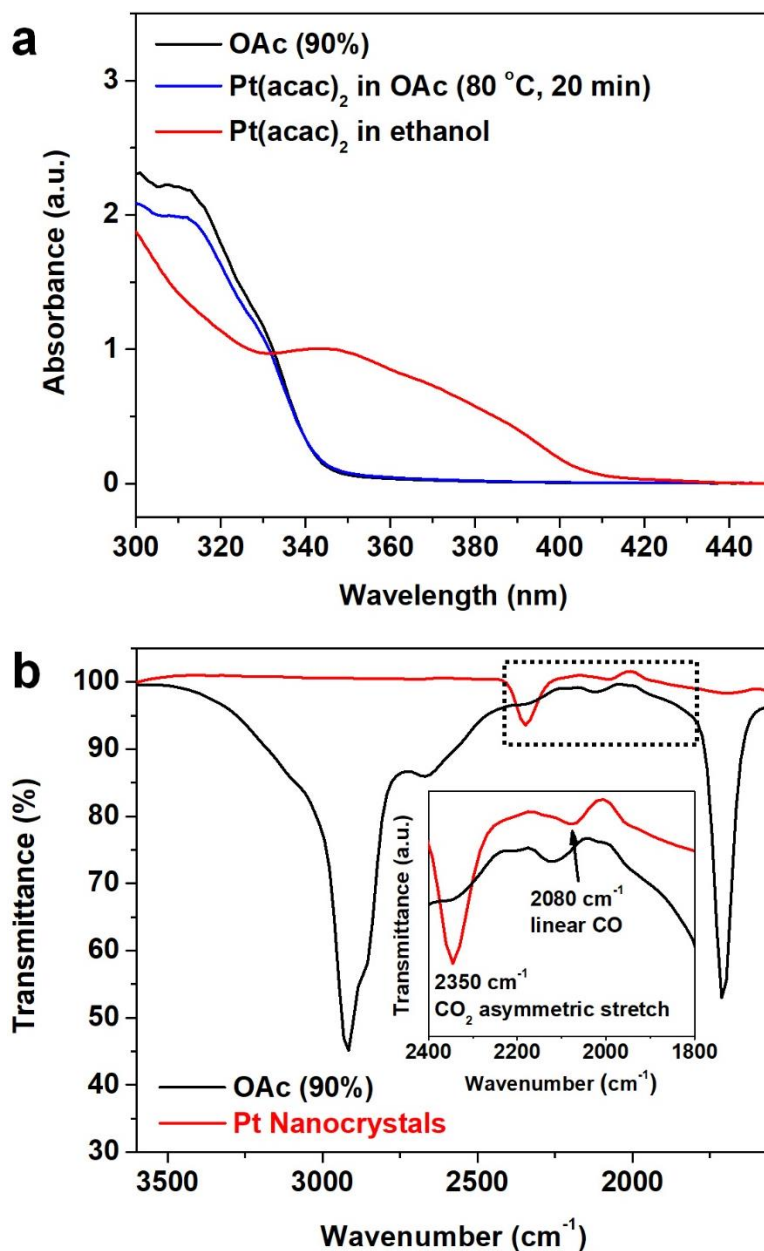


Figure 4. (a) UV-vis extinction spectra of Pt(acac)₂ in the presence of OAc (at a molar ratio of 5714 between OAc and Pt(acac)₂), with reference to OAc (90%) and a solution in ethanol. (b) FTIR spectra of the as-received OAc (90%) and the Pt nanocrystals prepared from OAc (90%).

In the nucleation stage, the OAc could serve as a surfactant to stabilize the nuclei and seeds by forming a densely-packed layer on the Pt surface through the involvement of elaidic acid—a conformational isomer of oleic acid.^[15] Further growth of the seeds led to the formation of

1
2
3
4
5 cubes/bars as the major product. Previous studies suggested that the presence of CO was pivotal
6
7 to the formation of Pt nanoscale cubes/bars because of its strong binding to the {100} facets.^[7a,16]
8
9 Therefore, we used FTIR to confirm the presence of CO adsorbed on the surface of the as-prepared
10
11 Pt cubes/bars. As shown in Figure 4b, the as-obtained Pt cubes/bars displayed an obvious CO band
12
13 at 2080 cm⁻¹, which can be assigned to linear binding.^[7a] Additionally, there was an obvious CO₂
14
15 band at 2350 cm⁻¹, corresponding to the asymmetric stretching mode.^[17] This peak can be
16
17 attributed to the possible decarboxylation of OAc under the condition used. The production of CO
18
19 was also confirmed by heating other metal precursors in OAc using a standard protocol. As shown
20
21 in Figure S3, Pd octahedral nanocrystals with edge lengths of 5-10 nm and Ir nanobars with an
22
23 average shorter edge length of 7 nm and an aspect ratio of 1.6 were generated after heating
24
25 Pd(acac)₂ and Ir(acac)₃ in OAc, respectively. The corresponding FTIR spectra also indicated the
26
27 adsorption of CO on the surface of the Pd and Ir nanocrystals (Figure S4). Taken together, it can
28
29 be concluded that OAc played multiple roles in the synthesis of Pt nanocrystals, including those
30
31 as a solvent, a ligand, and a stabilizer, as well as a precursor to CO that served as the actual reducing
32
33 agent and capping agent.
34

35
36 Figure 5 shows a general schematic for the formation of Pt cubes/bars with the assistance of
37
38 OAc at different stages. In the mixture containing Pt(acac)₂ and OAc used for the synthesis of Pt
39
40 nanocrystals, multiple types of reactions were involved. These reactions are summarized in Table
41
42 1. In the pre-nucleation stage, the ligand exchange between Pt(acac)₂ and OAc led to the generation
43
44 of Pt₃(OAc)₆ as a new Pt^{II} precursor. At an elevated temperature, the decarbonylation of OAc could
45
46 occur in the presence of the Pt^{II} complex, producing CO as a reducing agent for the generation of
47
48 atoms and a capping agent toward the Pt{100} facets. Once the Pt nuclei and seeds were formed,
49
50 they could serve as a catalyst for several reactions that only take place on the surface of Pt.^[14a,14c,18]
51
52 For example, as a stabilizer, OAc could chemically adsorb on the surface of the Pt nanocrystals
53
54 through the carboxyl group.^[19] With Pt surface as a catalyst, the carboxyl group in OAc could be
55
56 separated from the carbon chain due to decarbonylation and decarboxylation, leaving behind CO
57
58 and CO₂ molecules, respectively, on the surface of the nanocrystals. The CO molecules adsorbed
59
60
61
62
63
64
65

on the surface could promote the surface reduction of Pt^{II} precursor to continue the growth of the nanocrystals.

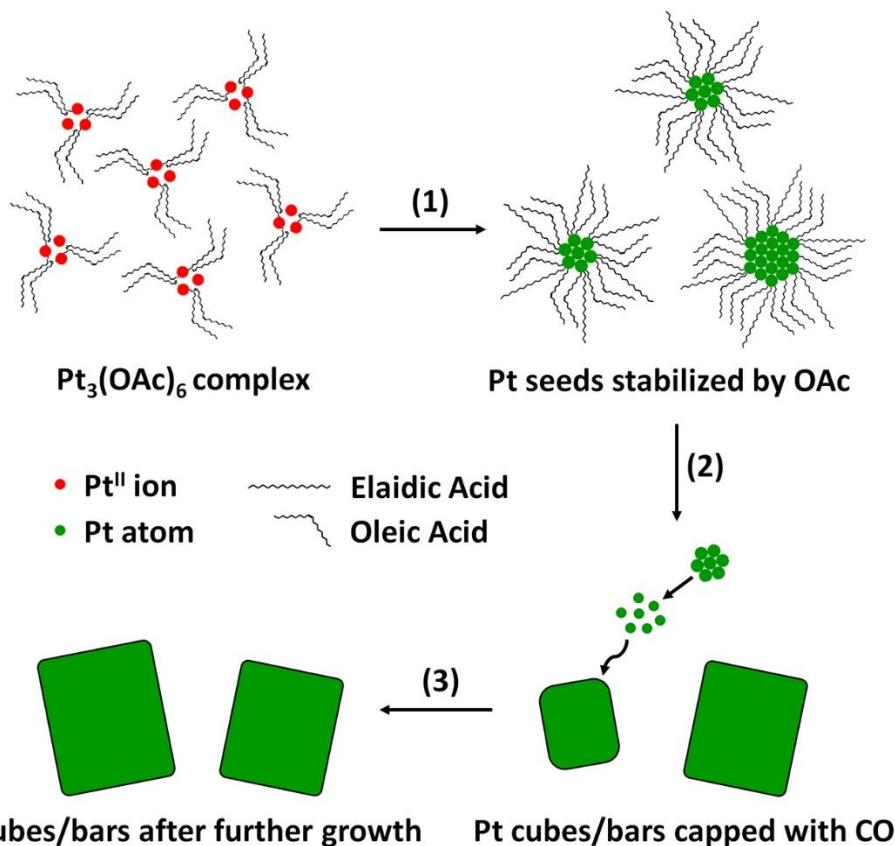


Figure 5. Schematic illustration showing the formation of Pt cubes/bars with the assistance of OAc: (1) formation of $\text{Pt}_3(\text{OAc})_6$ due to ligand exchange between $\text{Pt}(\text{acac})_2$ and OAc, reduction by the CO derived from decarbonylation of OAc, and creation of Pt seeds with OAc and elaidic acid densely packed on the surface to slow down the deposition of Pt atoms; (2) growth of the Pt seeds into cubes/bars with different sizes and capped by CO; and (3) occurrence of Ostwald ripening for the further growth of Pt cubes/bars at the expense of the smaller seeds.

Table 1. A summary of the possible reactions that could occur during different stages of a synthesis of Pt nanocrystals.

Stages	Reactions
--------	-----------

Pre-nucleation	Ligand Exchange: $3 \text{ Pt}(\text{acac})_2 + 6 \text{ C}_{17}\text{H}_{33}\text{COOH} \rightarrow \text{Pt}_3(\text{C}_{17}\text{H}_{33}\text{COO})_6 + 6 \text{ Hacac}$ Decarboxylation: $\text{C}_{17}\text{H}_{33}\text{COOH} \rightleftharpoons n\text{-C}_{17}\text{H}_{34} + \text{CO}_2$ Decarbonylation: $\text{C}_{17}\text{H}_{33}\text{COOH} \rightleftharpoons n\text{-C}_{17}\text{H}_{32} + \text{CO} + \text{H}_2\text{O}$ (primary)
Atom generation	$\text{CO} + \text{H}_2\text{O}(\text{g}) + \text{Pt}^{2+} \rightarrow \text{Pt}^0 + \text{CO}_2 + 2\text{H}^+$
Self-nucleation	$n \text{ Pt}^0 \rightarrow \text{Pt}_n^0$
Catalytic reactions on the surface of Pt	Water-gas shift reaction: $\text{CO} + \text{H}_2\text{O}(\text{g}) \rightarrow \text{CO}_2 + \text{H}_2$ Hydrogenation: $\text{H}_2 + \text{C}_{17}\text{H}_{33}\text{COOH} \rightarrow \text{C}_{17}\text{H}_{35}\text{COOH}$ Decarboxylation: $\text{C}_{17}\text{H}_{35}\text{COOH} \rightarrow n\text{-C}_{17}\text{H}_{36} + \text{CO}_2$ (primary) Decarbonylation: $\text{H}_2 + \text{C}_{17}\text{H}_{35}\text{COOH} \rightarrow n\text{-C}_{17}\text{H}_{36} + \text{CO}_{\text{ads}} + \text{H}_2\text{O}$ Deoxygenation: $3\text{H}_2 + \text{C}_{17}\text{H}_{35}\text{COOH} \rightarrow n\text{-C}_{18}\text{H}_{38} + 2\text{H}_2\text{O}$
Growth	$\text{CO}_{\text{ads}} + \text{H}_2\text{O}(\text{g}) + \text{Pt}_n^0 + \text{Pt}^{2+} \rightarrow \text{Pt}_{n+1}^0 + \text{CO}_2 + 2\text{H}^+$

Effects of the Experimental Parameters on both Size and Morphology. In an attempt to further expand the diversity of the products, we also investigated the effect of temperature on the size and morphology of the Pt nanocrystals. It was found that the product was transformed from 10-nm Pt cubes/bars to other types of nanocrystals with different sizes and shapes owing to alternations to the nucleation and growth processes (Figure 6). In one study, the reaction mixture was maintained at 80 °C for one week after ligand exchange. At this temperature, the OAc was relatively stable and could only generate a very limit amount of CO. In this case, the OAc was able to serve as a reducing agent, but providing a very weak reducing power under this mild temperature. The color of the reaction mixture did not change even after several days, indicating a very slow reduction rate for the Pt^{II} precursor under this condition. The final products contained nanocrystals without well-defined facets, together with a small fraction of Pt octahedral nanocrystals with an average edge length of 12 nm (Figure 6a). Because of the involvement of a slow nucleation process, there were also some nanocrystals featuring twin structures. In an effort to generate Pt nanocrystals with smaller size, we increased the reaction temperature from 120 °C to 140 °C and 210 °C to accelerate the nucleation and growth processes (Figure 6c and d). At these temperatures higher

than that was used in the standard protocol, the decarbonylation of OAc was promoted, producing more CO as a reducing agent and thus acceleration in nucleation. As a result, a large number of single-crystal seeds were formed, resulting in the formation of Pt cuboctahedral nanocrystals with an average size of about 5 nm.

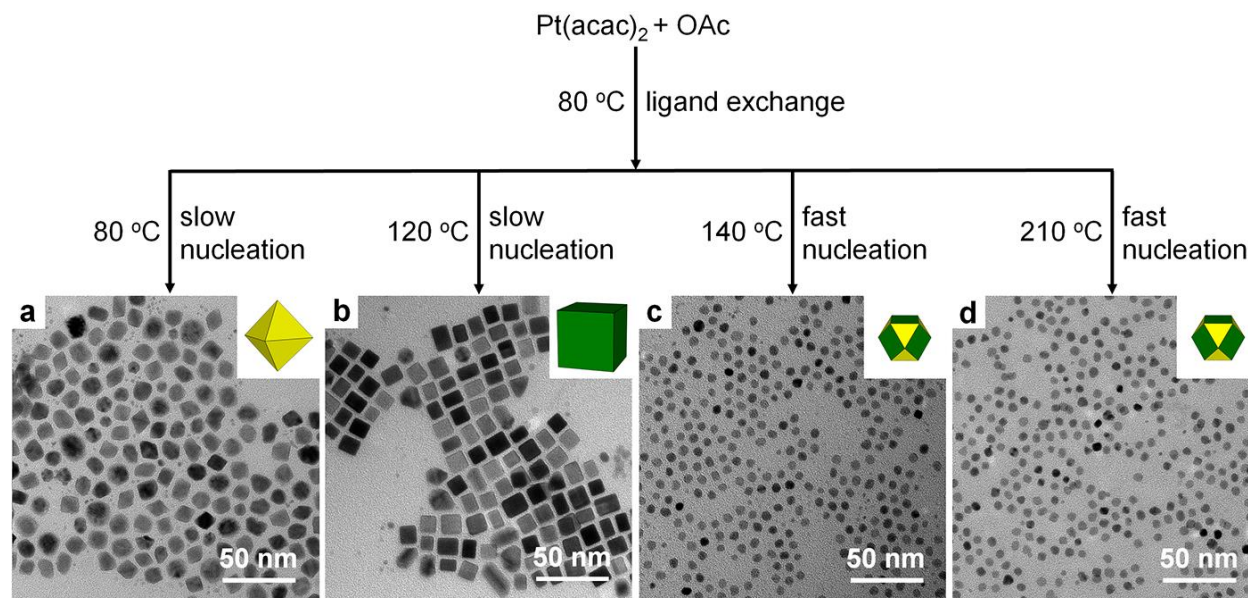


Figure 6. Schematic illustration showing the effect of reaction temperature on the size and morphology taken by the Pt nanocrystals. At 80 and 120 °C, the nucleation rate was relatively slow to generate a small number of seeds, resulting in the emergence of Pt octahedra with an average edge length of 12 nm and cubes/bars (cubes: 10 nm in edge length; bars: 8 nm in shorter edge length and an aspect ratio of 1.7), respectively. At 140 and 210 °C, the reduction rate was substantially increased, producing a relatively larger number of seeds and thus Pt cuboctahedra with a shorter edge length of about 5 nm.

Similar results were also obtained by changing the amount of the Pt^{II} precursor added into the reaction solution. As shown in [Figure S5a](#), when 1 mg of Pt(acac)₂ was used, the initial reduction rate of the Pt^{II} precursor was relatively slow due to a low concentration of the Pt^{II} precursor in the solution, producing truncated octahedral nanocrystals with an average edge length of about 6 nm. When the amount of Pt(acac)₂ was increased to 5 and 10 mg, 8-nm and 10-nm Pt cubes became

the dominant products, respectively (Figure S5b and c). A further increase in the amount of Pt(acac)₂ to 20 mg resulted in the formation of 5-nm Pt cuboctahedral nanocrystals (Figure S5d). Taken together, the diversity of the products could be expanded by tuning the reaction temperature and/or the molar ratio between Pt(acac)₂ and OAc.

Conclusion

In summary, we have conducted a set of experiments to elucidate the roles played by OAc at different stages in the formation of Pt nanocrystals using a simple protocol that only involved heating Pt(acac)₂ in OAc. In the pre-nucleation stage, the OAc went through ligand exchange with Pt(acac)₂, generating a Pt^{II}–oleate complex as the actual precursor to Pt atoms. When heated at an elevated temperature, OAc underwent decarbonylation to produce CO as a strong reducing agent for the generation of Pt atoms. Once Pt nuclei and seeds had been formed, they could serve as a catalyst for a number of reactions that only took place on the surface of Pt. These reactions further produced CO for serving as a capping agent toward the preferential formation of Pt{100} facets on the nanocrystals. Finally, the nanocrystals could continuously grow into larger sizes through the autocatalytic, surface reduction of the Pt^{II} precursor. The diversity of the products could be expanded by changing the reaction temperature and/or the molar ratio between Pt(acac)₂ and OAc to control the nucleation and growth processes. Considering the wide use of OAc and other long-chain fatty acids in the oil-phase synthesis of metal nanocrystals, we believe this mechanistic study will provide guideline to the rational synthesis of metal nanocrystals with desired properties.

Experimental Section

Chemicals and Materials. Platinum(II) acetylacetonate (Pt(acac)₂, 99.99%), oleic acid (OAc, 90%) were obtained from Sigma-Aldrich. Note that the 90% purity of commercial OAc refers to the cis conformation rather than chemical composition. All chemicals were used as received without further purification.

Synthesis of 10-nm Pt Cubes/Bars and 5-nm Pt Cuboctahedra. In a standard synthesis of 10-nm Pt cubes/bars, Pt(acac)₂ (2 mg, 0.0051 mmol) was added into OAc (10 mL) hosted in a 20-mL vial. The vial was then capped and heated at 80 °C in an oil bath under magnetic stirring for 20 min to facilitate the ligand exchange between Pt(acac)₂ and OAc till an equilibrium state was reached. The vial was then heated to and maintained at 120 °C in an oil bath under magnetic stirring for 24 h. The solid product was collected by centrifugation at 13300 rpm for 10 min, washed once with toluene, and finally dispersed in toluene for further use. We synthesized 5-nm Pt cuboctahedra using the same protocol except for the increase of temperature to 140 °C.

Characterization. Transmission electron microscopy (TEM) images were taken using a Hitachi HT7700 microscope operated at 120 kV. The samples for TEM analysis were prepared by drop-casting the suspension of nanocrystals onto carbon-coated Cu grids and drying under ambient conditions. X-ray diffraction (XRD) pattern was obtained on an X'Pert PRO Alpha-1 diffractometer (PANalytical, Almelo, The Netherlands). Ultraviolet–visible (UV–vis) extinction spectra were recorded on a Cary 60 spectrometer (Agilent Technologies, Santa Clara, CA). Fourier-transform infrared (FTIR) spectra were recorded on a Varian 640 IR spectrometer (Agilent Technologies, Santa Clara, CA).

Acknowledgements

This work was supported in part by a grant from the NSF (CHE-1804970) and start-up funds from the Georgia Institute of Technology. TEM imaging and XRD analyses were performed at the Georgia Tech Institute for Electronics and Nanotechnology, a member of the National Nanotechnology Coordinated Infrastructure, which is supported by the NSF (Grant ECCS-1542174).

Conflict of interest

The authors declare no competing financial interest.

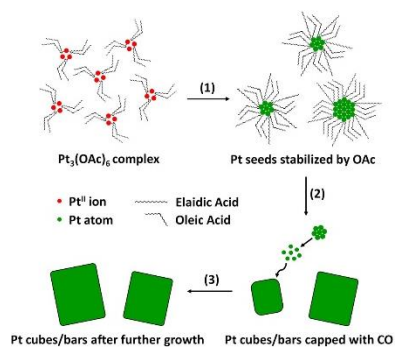
Keywords: oleic acid, nanocrystals, nucleation and growth, platinum

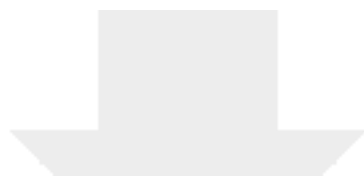
References

- [1] a) Z. Fan, H. Zhang, *Chem. Soc. Rev.* **2016**, *45*, 63–82; b) F. Bai, K. Bian, X. Huang, Z. Wang, H. Fan, *Chem. Rev.* **2019**, *119*, 7673–7717; c) E. C. Dreaden, A. M. Alkilany, X. H. Huang, C. J. Murphy, M. A. El-Sayed, *Chem. Soc. Rev.* **2012**, *41*, 2740–2779; d) J. P. Camden, J. A. Dieringer, J. Zhao, R. P. Van Duyne, *Acc. Chem. Res.* **2008**, *41*, 1653–1661.
- [2] a) Y. Xia, X. Xia, H. Peng, *J. Am. Chem. Soc.* **2015**, *137*, 7947–7966; b) A. Tao, S. Habas, P. Yang, *Small* **2008**, *4*, 310–325.
- [3] a) T. Yang, H. Peng, S. Zhou, C. Lee, S. Bao, Y. Lee, J. Wu, Y. Xia, *Nano. Lett.* **2017**, *17*, 334–340; b) Y. Wang, H. Peng, J. Liu, C. Huang, Y. Xia, *Nano. Lett.* **2015**, *15*, 1445–1450; c) M. Zhou, H. Wang, M. Vara, Z. D. Hood, M. Luo, T. Yang, S. Bao, M. Chi, P. Xiao, Y. Zhang, Y. Xia, *J. Am. Chem. Soc.* **2016**, *138*, 12263–12270; d) Y. Sun, *Chem. Soc. Rev.* **2013**, *42*, 2497–2511; e) M. Xie, S. Zhou, J. Zhu, Z. Lyu, R. Chen, Y. Xia, *Chem. Eur J* **2019**, *25*, 16397–16404.
- [4] R. Long, S. Zhou, B. J. Wiley, Y. Xiong, *Chem. Soc. Rev.* **2014**, *43*, 6288–6310.
- [5] a) X. Wang, M. Waje, Y. Yan, *J. Electrochem. Soc.* **2004**, *151*, A2183–A2188; b) X. Teng, X. Liang, S. Maksimuk, H. Yang, *Small* **2006**, *2*, 249–253; c) B. W. Lim, X. Lu, M. Jiang, P. H. C. Camargo, E. C. Cho, E. P. Lee, Y. Xia, *Nano. Lett.* **2008**, *8*, 4043–4047; d) C. Wang, H. Daimon, T. Onodera, T. Koda, S. Sun, *Angew. Chem. Int. Ed.* **2008**, *47*, 3588–3591.
- [6] W. Zhou, J. Wu, H. Yang, *Nano. Lett.* **2013**, *13*, 2870–2874.
- [7] a) B. Wu, N. Zheng, G. Fu, *Chem. Commun.* **2011**, *47*, 1039–1041; b) C. Lee, X. Yang, M. Vara, K. D. Gilroy, Y. Xia, *ChemNanoMat* **2017**, *3*, 879–884; c) L. Ruan, H. Ramezani-Dakhel, C. Y. Chiu, E. Zhu, Y. Li, H. Heinz, Y. Huang, *Nano. Lett.* **2013**, *13*, 840–846; d) M. Zhao, J. Holder, Z. Chen, M. Xie, Z. Cao, M. Chi, Y. Xia, *ChemCatChem* **2019**, *11*, 2458–2463; e) T. Yu, D. Y. Kim, H. Zhang, Y. Xia, *Angew. Chem. Int. Ed.* **2011**, *50*, 2773–2777.
- [8] Y. Kang, J. B. Pyo, X. Ye, R. E. Diaz, T. R. Gordon, E. A. Stach, C. B. Murray, *ACS Nano*

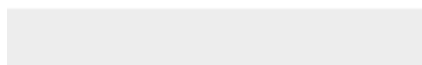
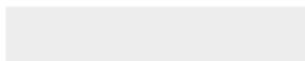
- 2013, 7, 645–653.
- [9] S. I. Choi, S. Xie, M. Shao, N. Lu, S. Guerrero, J. H. Odell, J. Park, J. Wang, M. J. Kim, Y. Xia, *ChemSusChem* **2014**, 7, 1476–1483.
- [10] X. Yin, M. Shi, J. Wu, Y. Pan, D. L. Gray, J. A. Bertke, H. Yang, *Nano. Lett.* **2017**, 17, 6146–6150.
- [11] a) S. Mourdikoudis, L. M. Liz-Marzan, *Chem. Mater.* **2013**, 25, 1465–1476; b) D. Baranov, M. J. Lynch, A. C. Curtis, A. R. Carollo, C. R. Douglass, A. M. Mateo-Tejada, D. M. Jonas, *Chem. Mater.* **2019**, 31, 1223–1230.
- [12] M. Watanabe, H. Takamura, H. Sugai, *Nanoscale Res. Lett.* **2009**, 4, 565–573.
- [13] a) A. C. Skapski, M. L. Smart, *Chem. Commun.* **1970**, 531, 658–659; b) I. J. S. Fairlamb, *Angew. Chem. Int. Ed.* **2015**, 54, 10415–10427.
- [14] a) M. Ahmadi, E. E. Macias, J. B. Jasinski, P. Ratnasamy, M. A. Carreon, *J. Mol. Catal. A–Chem.* **2014**, 386, 14–19; b) M. Ahmadi, A. Nambo, J. B. Jasinski, P. Ratnasamy, M. A. Carreon, *Catal. Sci. Technol.* **2015**, 5, 380–388; c) J. G. Immer, M. J. Kelly, H. H. Lamb, *Appl. Catal. A–Gen.* **2010**, 375, 134–139.
- [15] Y. Lu, X. Lu, B. T. Mayers, T. Herricks, Y. Xia, *J. Solid State Chem.* **2008**, 181, 1530–1538.
- [16] Y. Kang, X. Ye, C. B. Murray, *Angew. Chem. Int. Ed.* **2010**, 49, 6156–6159.
- [17] a) J. A. G. Castano, A. Fantoni, R. M. Romano, *J. Mol. Struct.* **2008**, 881, 68–75; b) G. Moore, A. Chizmeshya, P. F. McMillan, *Geochim. Cosmochim. Acta* **2000**, 64, 3571–3579.
- [18] J. Fu, X. Lu, P. E. Savage, *ChemSusChem* **2011**, 4, 481–486.
- [19] A. Neitzel, Y. Lykhach, V. Johaneck, N. Tsud, T. Skala, K. C. Prince, V. Matolin, J. Libuda, *J. Phys. Chem. C* **2014**, 118, 14316–14325.

Table of Contents





Click here to access/download
Supporting Information
chem.202003202-si.docx





Younan Xia, Ph.D.
*Brock Family Chair and GRA Eminent Scholar
The Wallace H. Coulter Department of
Biomedical Engineering*

August 11, 2020

Re: chem.202003202

Dr. Anne Deveson
Deputy Editor of *Chemistry – A European Journal*

Dear Anne,

Many thanks for your e-mail dated August 3, 2020. We have revised our manuscript by taking into account all the suggestions and comments from you and the two reviewers. All changes are highlighted with yellow pen in the review-only copy of the revised manuscript. Here we would like to specifically address the concerns from the reviewers.

Reviewer #1

Recommendation: Publish after minor revisions noted.

“In this manuscript, the authors elucidated the systematic study of role with oleic acid (OAc) in the nucleation and growth pathway. This manuscript has intensively investigated the effective role of OAc as a surfactant and reducing agent by FT-IR, UV-visible, TEM analysis, and controlled experiments. They showed that CO can be generated from OAc through a series of chemical reactions such as the dehydrogenation reaction, water-gas shift reaction, and decarbonylation process. As produced CO acts as a reducing agent and a surface stabilizer for (100) facet of Pt. Explaining the mechanism and the role of conventional surfactants is crucial in this field to understand overall nanoparticle synthesis in wet chemistry. Therefore, the paper is providing many scientific contents that are significant in the community of nanoscience. Below are comments/questions, which can be addressed during the revision process.”

1) “On page 5 in the manuscript, the authors explained that the diversity of the nanocrystal morphologies was ascribed to the multiple nucleation events. Recently, studies have reported that similar issues can be caused by impurities in commercial solvents. The presence of eladic acid, conformation isomer of OAc, can result in the inhomogeneity of nanocrystal morphology. It might be worth citing a recent report from Jonas and coworkers discussing the influence of impurity of commercial solvents. (Chem. Mater., 2019, 31, 4, 1223-1230).”

Response: We thank the reviewer for raising an excellent point. We have added the discussion and cited the reference about the potential impact of impurities in commercial solvents on the

diversity of the nanocrystals to the revised manuscript (see page 5 and ref. 11b).

2) *“The results for the reaction of Pt under OAc is intriguing. The authors showed that CO generated from OAc can trigger the reduction of Pt precursor. Despite the evidence for the specific steps with FT-IR, I suggest the author test at least a few other possible metal precursors here to show more cases. The authors mentioned the synthesis of Pd nanocrystals according to the previous reports of reference [3b]. However, the solvent in reference [3b] is not the OAc, but ethylene glycol.”*

Response: We thank the reviewer for the constructive suggestion. We have used other metal precursors including Pd(acac)₂ and Ir(acac)₃ under the same experimental condition and collected the FTIR spectra of the resultant Pd and Ir nanocrystals to confirm the generation and adsorption of CO. We have added the discussion to the revised manuscript (see page 12), together with the TEM and FTIR data to the Supporting Information as Figure S3 and S4.

For the reference 3b, although it reports the synthesis of Pd nanocrystals in ethylene glycol, the conclusion about the relationship between the initial reduction rate of the Pd^{II} precursor and the internal structure of the Pd seeds should be universal for the synthesis of noble-metal nanocrystals under different experimental conditions.

3) *“On page 10, The authors mentioned that the stretching mode of =C-H in Figure S2 decreased after the reaction at 80 °C. However, there is no corresponding data shown at 80 °C but only 120 °C in Figure S2. Therefore, the argument of the stretching modes is somewhat inconsistent.”*

Response: We thank the reviewer for his/her careful examination of our manuscript. We have corrected the inconsistent description in the revised manuscript (see page 10).

4) *“The description of the decomposition mechanism of OAc on page 10 should be reconsidered and revised. The authors mentioned that “Under the experimental conditions, the H₂ gas can only be generated through the decarbonylation of OAc, followed by water-gas shift reaction”. In the cited reference with Table 1, H₂ gas is generated through water-gas shift reaction rather than the decarbonylation of OAc. It is somewhat inconsistent that makes it hard to grab the key points of the mechanism.”*

Response: We understand the concern of this reviewer. Under the experimental condition of the present work, the H₂ gas can only be generated through water-gas shift reaction, which requires CO and H₂O as the reactants. Since the initially added chemicals only included Pt(acac)₂ and OAc, the CO and H₂O can only be produced through the decarbonylation of OAc. Therefore, we argued that decarbonylation of OAc led to the formation of H₂ gas, which is responsible for the subsequent hydrogenation of OAc.

Reviewer #2

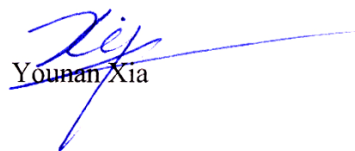
Recommendation: Publish as is; no revisions needed.

“This paper described a detailed and systematic study on the role of Oleic acid (OAc) on the synthesis of Pt nanocrystals. The results reported in this paper are important because it elucidates critical mechanistic aspects related to the role of OAc during the nucleation and growth stages of the synthesis, paving the way to the development of improved strategies for the tightly controlled synthesis of nanocrystals with target sizes and shapes. I believe the paper is of high quality and significance. It is also well written and the discussion is appropriately supported by the data. I recommend publication as it is.”

Response: We thank the reviewer for his/her candid assessment of our work.

We have also made some additional editorial changes to further enhance the quality of our paper. It is hoped the revised manuscript is now in the right format for publication in *Chemistry – A European Journal*.

Sincerely yours,


Younan Xia